Prepared for submission to JHEP SI-HEP-2018-27,CP3-18-55,MCnet-18-21

Measuring B anomalies by $\mu^+\mu^- \to t\bar{c}$ at future lepton colliders

Sichun Sun[a] **Qi-Shu Yan**[b,c] **Xiaoran Zhao**[d] **Zhijie Zhao**[c,e]

[a] *Department of Physics, National Taiwan University, Taipei, Taiwan*
[b] *School of Physics Sciences, University of Chinese Academy of Sciences, Beijing 100039, China*
[c] *Center for Future High Energy Physics, Institute of High Energy Physics, Chinese Academy of Sciences, Beijing 100039, China*
[d] *Dipartimento di Matematica e Fisica, Università di Roma Tre and INFN, sezione di Roma Tre, I-00146 Rome, Italy*
[e] *DESY, Notkestr. 85, 22607 Hamburg, Germany*

E-mail: sichunssun@gmail.com, yanqishu@ucas.ac.cn, xiaoran.zhao@uniroma3.it, zhijie.zhao@desy.de

Abstract: Being motivated from B anomalies, we study the match procedure of operators in the effective Hamiltonian in mass eigenstates and operators in the weak eigenstates. It is noticed that there are more operators in the SMEFT which can not simply being fixed from the low energy data from the B anomalies. We demonstrate this matching procedure with some new physics models, like Z' model and leptoquark models, and then consider how to probe these operators of SMEFT by using the process $\mu^+\mu^- \to tc$ at future muon colliders, which can provide complementary information on the underlying models which lead to B anomalies. We have performed a simple Monte Carlo simulation to show how to separate the signal events from the SM background events, and have estimated the sensitivity to the Wilson coefficients for different models.

Contents

1 Introduction 1

2 Matching and RGE of different operator bases 3

3 The Matching Conditions of New Physics 6

4 Signatute of $\mu^+\mu^- \to t\bar{c}$ at future muon colliders 8

5 Summary and Discussion 13

A SMEFT Renormalization Group Equation 14

B LEFT Renormalization Group Equation 15

1 Introduction

Searching for new physics is the prime target of both high energy frontier and high precision frontier. In the rare decays of B mesons, there exist long standing discrepances between the Standard Model predictions and experimental measurements, with a hint of non-lepton flavor universality(LFU), especially in the muon related final states. These B-anomalies are observed in a $B \to K\mu^+\mu^-$, $B_s \to \phi\mu^+\mu^-, B_s \to \mu^+\mu^-$ and angular distribution of $B \to K^*\mu^+\mu^-$[1–5]. For the LFU violation, it has been observed by LHCb[6–11] in the ratio

$$R_K = \frac{BR(B \to K\mu^+\mu^-)}{BR(B \to Ke^+e^-)}, R_{K^*} = \frac{BR(B \to K^*\mu^+\mu^-)}{BR(B \to K^*e^+e^-)} \tag{1.1}$$

Altough large hadronic uncertainties can enter in some of these absolute branching fractions and angular observables for the Standard model predictions, $R_K, R_{K^*}, B_s \to \mu^+\mu^-$ are considered relatively theoretically clean. The deviation in those measurements might lead to indirect evidence for new physics [12–20]. While those measurement provides derivation from SM prediction, the exact mechanics behind those anomaly are still unknown, and low-energy measurement couldn't fully reveal the nature behind that.

On the other hand, by scattering high energy particles, collider experiments provide unique opportunities to access underlying UV theories. Among various current and future colliders[21], a multi-TeV muon collider[22, 23] is ideal for such studies. Being fundamental particles, the entire energy of incoming muons are available to produce short-distance scattering rather than being spread among partons of hadrons, and thus a 14 TeV muon collider could be as effective as a 100 TeV proton-proton collider[24]. Such high energy

reach strongly benefits to searching new heavy particles, such as minimal dark matter models[25, 26], as well as indirect measurement at high energies[27]. Moreover, vector boson fusion processes are found to be important at muon colliders[28], and enable access to difficult parameters such as the Higgs quartic self-coupling[29]. More importantly, muon colliders have a special feature: the initial states are muons, directly related to those low-energy anomalies. The muon $g-2$ anomaly could be probed directly at muon colliders[30], In the context of muon $g-2$ anomaly, studies have been performed on testing it under the SMEFT formalism[30], and model-exhaustive analysis[30–33].

The multi-TeV reach and better precision advantages of muon colliders, makes a perfect place to probe muon related B anomalies in low energy. There are already proposals studying $\mu^+\mu^- \to b\bar{s}$ or $\bar{b}s$ at multi TeV scale to discuss the impact of low energy B-anomalies impact [34, 35]. At the current stage, B-anomalies can be nicely accommodated by effective four-fermion operators at B-physics scale ($\mu = 4.8$ GeV):

$$O_9 = (\bar{s}\gamma_\mu P_L b)(\bar{\ell}\gamma^\mu \ell), \tag{1.2}$$

$$O_{10} = (\bar{s}\gamma_\mu P_L b)(\bar{\ell}\gamma^\mu \gamma_5 \ell), \tag{1.3}$$

For the new physics effects described by operators O_9 and O_{10}, when we go above the weak scale ($\mu = M_Z$ for instance), the Wilson coefficients of such two operators depend on the specific models (e.g. leptoquark, scalars,Z',etc).

In this work, we adopt the same assumption that the new physics scale is around $\mu = 35$ TeV and it is challenging to discover the new physics signature at the LHC. We also assume that these new physics above the weak scale ($\mu = M_Z$) can be described by the framework of the standard model effective field theory (SMEFT). Under appropriate assumptions, it is noteworthy that there are at least one more operator is needed in order to match the SMEFT to low energy operators O_9 and O_{10}. These three operators in the SMEFT are given in Eqs. (2.12-2.14). Different new physics models can lead to different matching conditions across the weak scale.

Different from the proposal presented in [34], where the polarization of muon beams and charge tagging of jets in the final state are assumed, in this work, in order to reveal the nature of new physics which leads to the B anomalies, we propose to measure the process $\mu^+\mu^- \to tc$ (here tc denotes both $t\bar{c}$ and $\bar{t}c$), which can provide complementary information to the processes $\mu^+\mu^- \to b\bar{s}$ ($\bar{b}s$). The four fermion operators for $\mu^+\mu^- \to tc$ naturally arise from the operator matching conditions from low energy effective field theory to the SMEFT, since left-handed top and charm quarks form an electroweak SU(2) doublets as the partners of the left-handed bottom and strange quarks in SMEFT operators. We can also observe that the process $\mu^+\mu^- \to tc$ can help to distinguish different new physics models, which can yield different operator matching conditions. We will consider a Z' model and a few leptoquark models.

The leptoquark particles are predicted in the grand unification models and they could either be scalar or vector bosons. Usually, these particles should be superheavy (say 10^13 GeV), as required by the experimental data of proton decays. Very light leptoquarks (say 1 TeV or a few 10 TeV) can be consistent with experimental data if their couplings to

the first generation of matter fields are weak. Light leptoquarks are also predicted in the Pati-Salam model, where lepton numbers are treated as the forth color quantum number. These light leptoquarks could be even accessible at the LHC and future collider projects. Recently, leptoquarks have attracted much attentions in order to interpret the B anomalies. A comprehensive on the phenomenology of leptoquark can be found in [36].

Our main findings Our new findings include: 1) The dominant background events of the SM for the process $\mu^+\mu^- \to tc$ are different from those of the process $\mu^+\mu^- \to bs$. Due to the highly boosted top quark in the final states, jet substructure analysis can be crucial to distinguish signal and background events. 2) In the case that there is no new resonance which will be found the TeV muon colliders, measurement of the process $\mu^+\mu^- \to tc$, can provide crucial information on the potential nature of the new physics which leads to the low energy B anomalies. 3) The weak final state radiation might become important for such a measurement.

This paper is organized as given below. In section II, we demonstrate the relations between the Wilsonian coefficients of the effective Hamiltonian and those of the SMEFT. In section III, we present the values of Wilsonian coefficients of the SMEFT derived from different new physics models. These new physics models can accommodate the data of B anomalies. In section IV, we perform a Monte Carlo simulation to explore the sensitivity of future muon colliders to these new physics scenarios. We end this work with a few discussion and conclusion. In Appendix, we present the renormalization group equations of Wilsonian coefficients in the SMEFT and effective Hamiltonian, respectively.

2 Matching and RGE of different operator bases

Interestingly, these anomalies can be simultaneously explained in form of a model-independent way with the effective four-fermion operators. In many researches of B-physics, new physics effects strongly prefer an effective Hamiltonian with O_9 and O_{10} with Wilson coefficients of dimension 6 interactions at the renormalization scale $\mu = 4.8$ GeV ,

$$\mathcal{H}_{eff} = \mathcal{H}_{eff}^{SM} - \mathcal{N} \sum_{\ell=e,\mu} \sum_{i=9,10} \left(c_i O_i^{bs\ell\ell} + c_i' O_i'^{bs\ell\ell} \right) + h.c., \tag{2.1}$$

where the normalization factor $\mathcal{N}$ is

$$\mathcal{N} = \frac{4G_F}{\sqrt{2}} V_{tb} V_{ts}^* \frac{e^2}{16\pi^2}. \tag{2.2}$$

The operators O_9 and O_{10} are

$$O_9^{bs\ell\ell} = (\bar{s}\gamma_\mu P_L b)(\bar{\ell}\gamma^\mu \ell), \tag{2.3}$$

$$O_{10}^{bs\ell\ell} = (\bar{s}\gamma_\mu P_L b)(\bar{\ell}\gamma^\mu \gamma_5 \ell), \tag{2.4}$$

where $P_L = (1 - \gamma_5)/2$ is the left-handed projection operator. For O_i', P_L is replaced by right-handed projection operator $P_R = (1 + \gamma_5)/2$.

For the purpose of this paper, to study B-anomalies related operator O_9 and O_{10} defined in the low energy B physics scale in higher colliding energy scale, we need to treat the

running and matching of the operators carefully. Especially the subtleties arise when the energy running across the weak scale. Our study finds that in the energy scale above the weak scale, the impact of O_9 and O_{10} operators needs to be reparametrized by three different operators, rather than two, in so-called Warsaw basis, known as the Standard model effective theory (SMEFT). Here we introduce different basises and coefficient matching as below.

At the scale below the weak scale, potential new physics effects are described by a low energy effective field theory (LEFT). The LEFT Lagrangian with dimension 6 operators can be written as

$$\mathcal{L}_{LEFT} = \mathcal{L}_{QCD+QED} + \frac{1}{v^2}\sum_i L_i Q_i,$$

where L_i are the Wilson Coefficients of LEFT, and $v = 246$ GeV is the vacuum expectation value.

In this paper, we use the convention of Ref. [37]. The most relevant operators are

$$Q_{ed}^{V,LL}(p,r,s,t) = (\bar{e}_{Lp}\gamma^\mu e_{Lr})(\bar{d}_{Ls}\gamma_\mu d_{Lt}), \tag{2.5}$$
$$Q_{de}^{V,LR}(p,r,s,t) = (\bar{d}_{Lp}\gamma^\mu d_{Lr})(\bar{e}_{Rs}\gamma_\mu e_{Rt}), \tag{2.6}$$

where p, r, s, t are generation indices of quark or lepton. Since the EW symmetry is broken, here e and d are the lepton field and down-type quark field. L and R are the chiral indices of fermions.

One can derive the relations between Q_i and O_i easily:

$$Q_{ed}^{V,LL} = \frac{1}{2}\left(O_9 - O_{10}\right), \tag{2.7}$$
$$Q_{de}^{V,LR} = \frac{1}{2}\left(O_9 + O_{10}\right). \tag{2.8}$$

So we have

$$L_{ed}^{V,LL} = \frac{\mathcal{N}v^2}{2}(c_9 - c_{10}), \tag{2.9}$$
$$L_{de}^{V,LR} = \frac{\mathcal{N}v^2}{2}(c_9 + c_{10}). \tag{2.10}$$

The constraints of c_9 and c_{10} can be found in Ref. [38].

Assuming the new physics appears at a scale above the weak scale Λ, the SMEFT Lagrangian with dimension 6 operators ($\mathcal{O}_i$) is defined as

$$\mathcal{L}_{SMEFT} = \mathcal{L}_{SM} + \frac{1}{\Lambda^2}\sum_i C_i \mathcal{O}_i, \tag{2.11}$$

where C_i are called Wilson Coefficients.

A complete set of non-redundant dimension 6 operators has been derive in Ref. [39], so-called Warsaw basis. The most relevant operators in this paper are

$$\mathcal{O}_{lq}^{(1)}(p,r,s,t) = (\bar{l}_p\gamma^\mu l_r)(\bar{q}_s\gamma_\mu q_t), \tag{2.12}$$
$$\mathcal{O}_{lq}^{(3)}(p,r,s,t) = (\bar{l}_p\gamma^\mu \tau^I l_r)(\bar{q}_s\gamma_\mu \tau^I q_t), \tag{2.13}$$
$$\mathcal{O}_{qe}(p,r,s,t) = (\bar{q}_p\gamma^\mu q_r)(\bar{e}_s\gamma_\mu e_t), \tag{2.14}$$

	$c_9 = -0.73, c_{10} = 0$	$c_9 = 0, c_{10} = 0.54$	$c_9 = c_{10} = 0.05$	$c_9 = -c_{10} = -0.39$
$L_{ed}^{V,LL}(m_B)$	-1.727×10^{-5}	-1.278×10^{-5}	0	-1.845×10^{-5}
$L_{ed}^{V,LL}(m_Z)$	-1.748×10^{-5}	-1.287×10^{-5}	5.651×10^{-9}	-1.863×10^{-5}
$(C_{lq}^{(1)} + C_{lq}^{(3)})(m_Z)$	-0.029	-0.021	9.337×10^{-6}	-0.031
$(C_{lq}^{(1)} + C_{lq}^{(3)})(\Lambda)$	-0.030	-0.023	2.053×10^{-5}	-0.032
$L_{de}^{V,LR}(m_B)$	-1.727×10^{-5}	1.278×10^{-5}	2.366×10^{-6}	0
$L_{de}^{V,LR}(m_Z)$	-1.723×10^{-5}	1.268×10^{-5}	2.355×10^{-6}	-4.408×10^{-8}
$C_{qe}(m_Z)$	-0.028	2.096×10^{-2}	3.891×10^{-3}	-7.283×10^{-5}
$C_{qe}(\Lambda)$	-0.029	2.142×10^{-3}	3.993×10^{-3}	-2.019×10^{-4}

Table 1. The coefficients $L_{ed}^{V,LL}$, $L_{de}^{V,LR}$, $C_{lq}^{(1)} + C_{lq}^{(3)}$ and C_{qe} at scale $m_B = 5$ GeV, $m_Z = 91.1876$ GeV and $\Lambda = 10$ TeV are listed, with difference input of c_9 and c_{10}. Here, we assume $C_{lq}^{(1)} = 3C_{lq}^{(3)} = \frac{3}{4} L_{ed}^{V,LL} \times \Lambda^2/v^2$.

where q, l, e are the left-handed quark doublet, left-handed lepton doublet, and right-handed lepton singlet, respectively. p, r, s, t are generation indices of quark or lepton.

When the electroweak symmetry breaking occurs, the SM heavy particles (top, Higgs, $W^{\pm}$, Z) are integrated out, and the SMEFT should be matched to LEFT. The full matching conditions at tree level have been derived by Ref. [37]. In this paper, we only consider the operators with flavour indices $(p, r, s, t) = (2, 2, 2, 3)$ or $(p, r, s, t) = (2, 3, 2, 2)$, so the matching conditions are simplified to

$$L_{ed}^{V,LL}(2,2,2,3) = \frac{v^2}{\Lambda^2}\left[C_{lq}^{(1)}(2,2,2,3) + C_{lq}^{(3)}(2,2,2,3)\right], \tag{2.15}$$

$$L_{de}^{V,LR}(2,3,2,2) = \frac{v^2}{\Lambda^2} C_{qe}(2,3,2,2). \tag{2.16}$$

The related renormalization group equations for the SMEFT and LEFT can be found in the Appendix A and Appendix B, respectively.

3 The Matching Conditions of New Physics

At muon colliders, the operators we input are actually Eq. (2.14). In massless limit,[1] the differential cross section for $\mu^+\mu^- \to tc$ and $\mu^+\mu^- \to bs$ are:

$$\frac{\mathrm{d}\sigma(\mu^+\mu^- \to X)}{\mathrm{d}\cos\theta} = \frac{3s}{256\pi} |C_{LL}^X|^2 (1 + \cos\theta)^2 \tag{3.1}$$

where

$$C_{LL}^{bs} = C_{lq}^{(1)} + C_{lq}^{(3)}, C_{LL}^{tc} = C_{lq}^{(1)} - C_{lq}^{(3)} \tag{3.2}$$

[1]For simplicity, in this section we work under massless limit. Nevertheless, for the numerical results discussed in later sections, full mass dependence are included

Integrating over $\cos\theta$, we can obtain the inclusive cross section as:

$$\sigma(\mu^+\mu^- \to X) = \frac{1}{32\pi} s |C_{LL}^X|^2 \tag{3.3}$$

In a general new physical model, both $C_{lq}^{(1)}$ and $C_{lq}^{(3)}$ can be non-zero, and thus both processes $\mu^+\mu^- \to tc$ and $\mu^+\mu^- \to bs$ receives new physical contribution, and can be measured in future muon colliders. We note that for $\mu^+\mu^- \to bs$, the corresponding Wilson coefficients C_{LL}^{bs} is directly in charge of $b \to s\mu^+\mu^-$ transition in B-physics, and hence constrained by those measurements. On the other hand, C_{LL}^{tc} is unconstrained. As a general argument, the underlying new physical which induce C_{LL}^{bs} or equivalently $C_{lq}^{(1)}, C_{lq}^{(3)}$, would induce also C_{LL}^{tc} with size at similar order.

Therefore, we expect that the cross section of $\mu^+\mu^- \to tc$ is comparable to $\mu^+\mu^- \to bs$, and as we will show in Section 4, due to the presence of top quark in the final state of $\mu^+\mu^- \to tc$, it is easier to measure than $\mu^+\mu^- \to bs$. To be more specific, below we discuss four types of new physics models labelled as Model I-IV, where the relations between C_{LL}^{tc} and C_{LL}^{bs} are given, and later in Section 4 we will show how to distinguish them by measuring both $\mu^+\mu^- \to tc$ and $\mu^+\mu^- \to bs$.

Model I A Z' mdoel with flavor symmetry $U(1)_{L_\mu - L_\tau}$. In this model, the $L_\mu - L_\tau$ is promoted into a $U(1)$ gauge symmetry, which is mediated by a massive gauge boson Z'. Originally it was proposed for muon $g-2$ anomaly [40] and neutrino mixing [41]. Later it is realised that its coupling to quarks can be described by high dimensional operators, which can be generated through new heavy quarks [42]. Such interaction can induce flavor violation [43], to explain B anomaly. Since the effective interaction between $bs\mu\mu(tc\mu\mu)$ is mediated by an s-channel Z', which is an electroweak singlet, clearly $C_{lq}^{(3)} = 0, C_{LL}^{bs} = C_{LL}^{tc} = C_{lq}^{(1)}$. Consequently, we have $\sigma(tc) \sim \sigma(bs)$.

Model II A scalar triplet leptoquark S_3 model. In this model, the new physics are mediated by a heavy scalar leptoquark, which belongs to $SU(2)_L$ triplet. The corresponding Lagrangian can be written as [36]

$$\mathcal{L}_{NP} = \sum_{i,j} \lambda_{ij} \bar{Q}_i^c (i\tau^2) \tau^I L_j S_3^I + \text{h.c.} \tag{3.4}$$

In this model, both $C_{lq}^{(1)}$ and $C_{lq}^{(3)}$ can be generated at tree-level, which is given by [44]

$$[C_{lq}^{(1)}]_{prst} = 3\frac{\lambda_{sp}^* \lambda_{tr}}{4M^2} \tag{3.5}$$

$$[C_{lq}^{(3)}]_{prst} = \frac{\lambda_{sp}^* \lambda_{tr}}{4M^2}. \tag{3.6}$$

where M is the mass of the leptoquark S_3. Therefore, we have $C_{LL}^{bs} = 2C_{LL}^{tc}$, and $\sigma(tc) = \frac{1}{4}\sigma(bs)$

Model III A scalar singlet leptoquark S_1 model. In this model, new physics are mediated by a heavy scalar leptoquark, which belongs to $SU(2)_L$ singlet. There are three possible hypercharge assignments, and we consider the case $Y = \frac{1}{3}$ here. The corresponding Lagrangian is

$$\mathcal{L}_{NP} = \sum_{i,j} \lambda_{ij} \bar{Q}_i^c (i\tau_2) L_j S_1 + \text{h.c.} \tag{3.7}$$

At tree-level, the relevant Wilson coefficients are

$$[C_{lq}^{(1),\text{tree}}]_{prst} = \frac{\lambda_{sp}^{L*} \lambda_{tr}^{L}}{4M^2} \tag{3.8}$$

$$[C_{lq}^{(3),\text{tree}}]_{prst} = -\frac{\lambda_{sp}^{L*} \lambda_{tr}^{L}}{4M^2} \tag{3.9}$$

Interestingly, we can see that at tree-level $C_{LL}^{bs} = 0$. The leading contribution to C_{LL}^{bs} starts from one-loop level [45]. Consequently, we expect that $C_{LL}^{bs} \ll C_{LL}^{tc}$, and hence $\sigma(tc) \gg C_{LL}^{bs}$. For the experiment bounds($C_9 = -1$ benchmark point), we get

$$\sum_i |\lambda_{u_i\mu}|^2 \text{Re} \frac{(\lambda\lambda^\dagger)_{bs}}{V_{tb}V_{ts}^*} - 1.74|\lambda_{t\mu}|^2 \sim 12.5\hat{M}^2 \tag{3.10}$$

where $\hat{M}$ is the mass of the leptoquark in terms of unit TeV, and from $B_s - \bar{B}_s$ mixing we have

$$\frac{(\lambda\lambda^\dagger)_{bs}}{V_{tb}V_{ts}^*} \sim (1.87 + 0.45i)\hat{M} \tag{3.11}$$

For perturbativity, we have $|\lambda_{u_i\mu}|^2 < 4\pi$, which yield

$$M \lesssim 1.9\text{TeV} \tag{3.12}$$

Consequently, we expect that at the energy range of future muon colliders, it can be produced on-shell, and be observed directly.

Model IV A U_1 vector leptoquark model. Originally proposed in [46], see also [47]. The Lagrangian is given by

$$\mathcal{L}_{NP} = -\frac{1}{2} U_{1,\mu\nu}^\dagger U^{1,\mu\nu} + M_U^2 U_{1,\mu}^\dagger U_1^\mu + g_U U_{1,\mu} \lambda_{ij} \bar{Q}_i \gamma^\mu L_j + \text{h.c.} \tag{3.13}$$

The relevant Wilson coefficients are

$$[C_{lq}^{(1),\text{tree}}]_{prst} = g_U^2 \frac{\lambda_{sp}^{L*} \lambda_{tr}^{L}}{2M^2} \tag{3.14}$$

$$[C_{lq}^{(3),\text{tree}}]_{prst} = g_U^2 \frac{\lambda_{sp}^{L*} \lambda_{tr}^{L}}{2M^2} \tag{3.15}$$

Clearly, in this case we have $C_{LL}^{tc} \sim 0, C_{LL}^{bs} \gg C_{LL}^{tc}$.

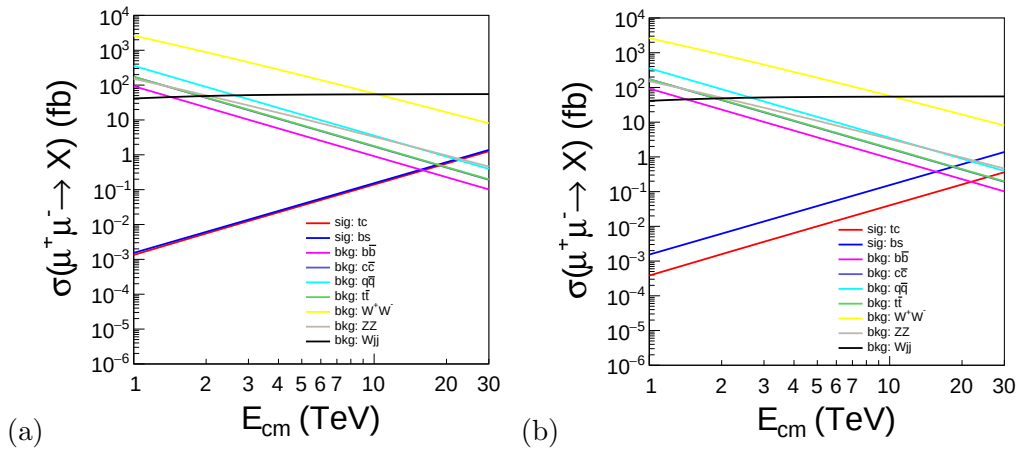

Figure 1. The energy dependencies of the cross sections of $\mu^+\mu^- \to X$ are displayed. For the signal, $X = t\bar{c}$, while X is the final state of the background. The best fits $c_9 = -c_{10} = -0.39$ in Ref. [38] have been considered here. Their values are evaluated to the cutoff $\Lambda = 10$ TeV by our RGEs and matching conditions in the Appendix. Two relations between $C_{lq}^{(1)}$ and $C_{lq}^{(3)}$ have been considered: (a) $C_{lq}^{(1)} = L_{ed}^{V,LL} \times \Lambda^2/v^2$ and $C_{lq}^{(3)} = 0$, and (b) $C_{lq}^{(1)} = 3C_{lq}^{(3)} = \frac{3}{4} L_{ed}^{V,LL} \times \Lambda^2/v^2$.

4 Signatute of $\mu^+\mu^- \to t\bar{c}$ at future muon colliders

To study the $\mu^+\mu^- \to t\bar{c}$ process at future muon collider, we generate a UFO model with relevant operators by Feynrules [48], and import it to Madgraph5_aMC@NLO[49]. We calculate the cross sections of signals and backgrounds from $E_{cm} = 1$ TeV to 30 TeV. The energy dependencies of the cross sections are shown in the Fig. 1. The main background processes include $b\bar{b}$, $c\bar{c}$,$q\bar{q}$ ($q = u, d, s$), $t\bar{t}$, W^+W^-, ZZ and $W^\pm jj$ ($j = u, d, s, c$). The process $W^\pm jj$ is also included because it describes the weak final state radiation. On one hand, backgrounds with two final states are from S-channel and decrease with the increase of the collision energy. On the other hand, the dominant contribution of $W^\pm jj$ is T-channel process, and its cross sections are almost the same with different E_{cm}.

The cross section of main signal process $\mu^+\mu^- \to t\bar{c}(\bar{t}c)$ derived from the 4-fermion interactions are proportional to collision s^2, and it increases with the increase of the collision energy, as shown in Fig. 1. The largest signal is the case that only c_9 is switched on, and it can reach $\mathcal{O}(1)$ fb at the 30 TeV.

Near the threshold, cross section of all background processes are huge when compared with the signal process. With the increase of collision energy, the signal cross section can even be larger than those of background processes if the collision energy is large enough (say $\sqrt{s} = 30$ TeV) for some new physics models. Nonetheless, when $\sqrt{s} = 10$ TeV, it might be still challenging to discover the signal events since the cross section of background processes are several orders larger than that of the signals processes.

In Fig. 1, the best fits of c_9 and c_{10} in Ref. [38] have been considered. Their values are evaluated to the EW scale by our RGEs Eq. B.1 and Eq. B.2. And then they are matched to SMEFT by Eq. 2.15 and Eq. 2.16. From Eq. 2.15, we also know that the constraint from

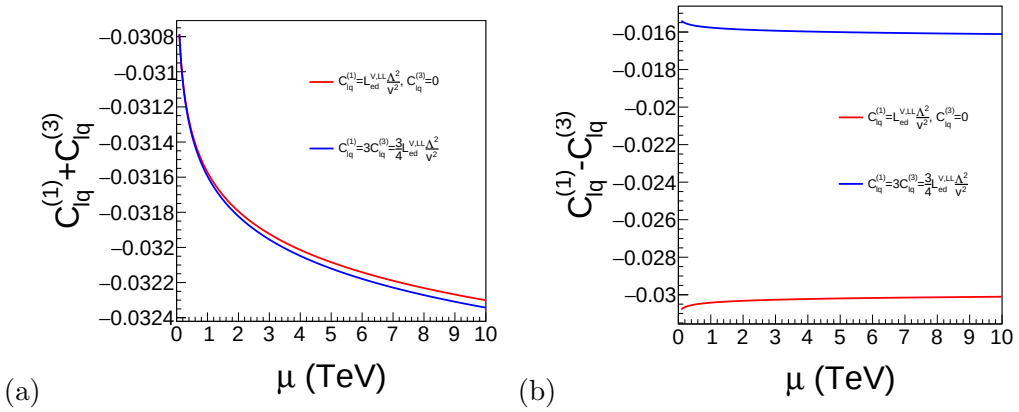

Figure 2. The running of (a) $C_{lq}^{(1)} + C_{lq}^{(3)}$ and (b) $C_{lq}^{(1)} - C_{lq}^{(3)}$ from EW scale to $\Lambda = 10$ TeV is display. Two scenarios: 1) $C_{lq}^{(1)} = L_{ed}^{V,LL}\Lambda^2/v^2$ and $C_{lq}^{(3)} = 0$, and 2) $C_{lq}^{(1)} = 3C_{lq}^{(3)} = \frac{3}{4}L_{ed}^{V,LL} \times \Lambda^2/v^2$ have been considered here.

B physics can be only applied to the sum of $C_{lq}^{(1)} + C_{lq}^{(3)}$ [2]. So any new physics scenarios with $C_{lq}^{(1)}$ and $C_{lq}^{(3)}$ as free parameters cannot be constrained by the data from B physics experiments. In Fig. 2, we show the running of $C_{lq}^{(1)}+C_{lq}^{(3)}$ and $C_{lq}^{(1)}-C_{lq}^{(3)}$ from EW scale to new physics scale at $\Lambda = 10$ TeV, in the case of $c_9 = -0.73$ and $c_{10} = 0$. We have considered two naive scenarios: 1) $C_{lq}^{(1)} = L_{ed}^{V,LL}\Lambda^2/v^2$, $C_{lq}^{(3)} = 0$, and 2) $C_{lq}^{(1)} = 3C_{lq}^{(3)} = 3L_{ed}^{V,LL}\Lambda^2/4v^2$. Obviously, it is hard to distinguish these two cases if we only know the value of $C_{lq}^{(1)} + C_{lq}^{(3)}$ by measuring $\mu^+\mu^- \to b\bar{s}(\bar{b}s)$. The measurement of $\mu^+\mu^- \to t\bar{c}(\bar{t}c)$ is also necessary to constrain the value of $C_{lq}^{(1)} - C_{lq}^{(3)}$.

As we have seen in Fig. 1, the process $\mu^+\mu^- \to t\bar{c}$ can only be observable when $E_{cm} > 10$ TeV. In such high energy, we can expect that two energetic jets are observed at the detector for either signal and background events. For the signal events, one jet with invariant mass around top mass and another one with invariant mass around charm mass [3]. While for other background events, such as W^+W^- and $t\bar{t}$, the invariant mass of boosted W and top quark can generate large jet mass when the cone parameter is large enough to include all their decay products. For background events, such as $q\bar{q}$, we expect jet mass should be small if the jet cone parameter is set to be appropriate.

To further investigate the kinematic features of signal and background, we generate events with $E_{cm} = 10$ TeV. We consider Model I with $c_9 = -c_{10} = -0.39$ as input, since it has a large cross section and the effects from C_{qe} can be ignored. All events are hadronic decayed by Madgraph5_aMC@NLO. And then we use PYTHIA8 [50] for parton shower and hadronization, and FastJet [51] to reconstruct jets. In the FastJet, we use the generalised k_t algorithm for e^+e^- collisions, which is extended from a simple k_t algorithm [52]. This

[2]The generation indices are always $(p, r, s, t) = (2, 2, 2, 3)$ for $C_{lq}^{(1)}$ and $C_{lq}^{(3)}$ and $(p, r, s, t) = (2, 3, 2, 2)$ for C_{qe} in this paper

[3]In our Monte Carlo simulation, the charm mass is set to zero

algorithm defines two distances:

$$d_{ij} = \min(E_i^{2p}, E_j^{2p}) \frac{1-\cos\theta_{ij}}{1-\cos R}, \tag{4.1}$$

$$d_{iB} = E_i^{2p}, \tag{4.2}$$

where p and R are input by user. If a d_{ij} is smallest then particle i and j are recombined, while d_{iB} is smallest then i is called an "inclusive jet".

The original k_t algorithm [52] only has a single distance:

$$d_{ij} = \min(E_i^2, E_j^2)\,(1-\cos\theta_{ij})\,, \tag{4.3}$$

which is identical to Eq. 4.1 by choosing $\pi < R < 3\pi$ and $p = 1$. In this case, one can extract "exclusive jet" only. For the high energy muon collider, muon beams may radiate energetic particles and have large angles to the beam. It is hard to include such kind of particles to beam jets. So this algorithm is not sufficient in our context.

The optimization of parameter p and R is a complicate task. As a first attempt, we choose $p = 1$ so it works similar to a k_t algorithm for hadron collider [53, 54]. For the $t\bar{c}(\bar{t}c)$ final state, we hope to find a R parameter to reconstruct a heavy jet around top mass and a light jet. We scan the R parameter from 0.05 to 0.15 and find that $R = 0.10$ can satisfy this requirement. In Fig. 3(a), we display the energy distribution of jets in $t\bar{c}(\bar{t}c)$ final with $R = 0.10$ and $p = 1$. These jets are sorted by energy. Obviously, the first two jets have energy around $E_{cm}/2$, which means that they are probably originated from the hard process. We can also observed that the energy of the 3th jet can reach several hundred GeV or TeV level. In such high energy collider, parton shower can radiate some high enery particles and can be detected as a hard jet. To reduce these radiations, we implement a cut $E(j) > 500$ GeV to events. After this cut, we plot the number of jets in Fig. 3(b). As we can see, the peak is $N_{jets} = 2$ for two final state process and the peak for $W^{\pm}jj$ background is 3.

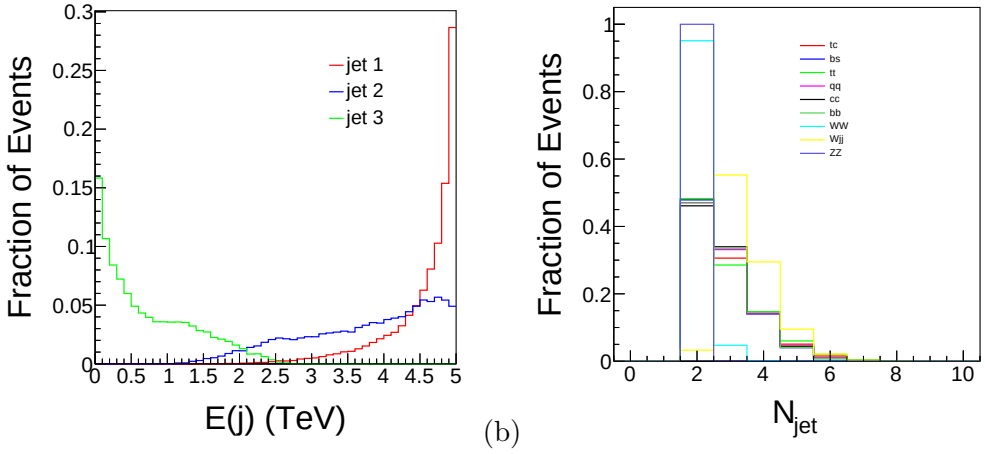

(a) (b)

Figure 3. (a) The jet energy distributions of process $\mu^+\mu^- \to t\bar{c}$ are displayed, where jets are sorted by energy. (b) The number of jets after implementing cut $E(j) > 500$ GeV.

Fig. 4 shows the invariant masses of the two most energetic jets of signal and backgrounds. Here, we label the heavy jet as HJ in Fig. 4(a) and the light one as LJ in Fig. 4(b). As we expect, HJ has a peak around top mass and the distribution of LJ is flat for the signal. For the backgrounds with heavy particles (t, W, and Z), we also observe peaks around their masses. It is because these particles are highly boosted in such high energy machine. We can include all their decayed products by choosing a small jet cone like $R = 0.10$.

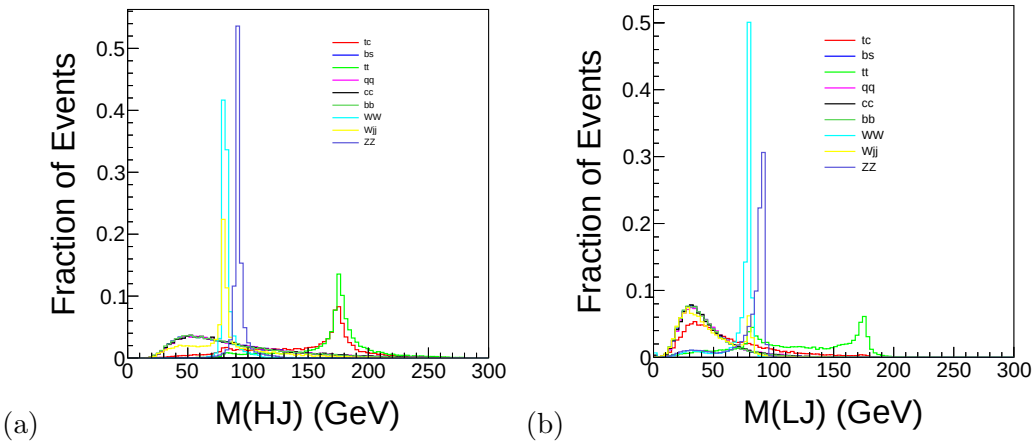

(a) (b)

Figure 4. The invariant mass of (a) the heavy jet and (b) the light jet in signal and backgrounds are displayed.

Since we only consider hadronic decay, top quark should decay to b quark and W boson, and W further decays to light quarks. So the HJ should be tagged as a b-jet in future detector. In this paper, the detector simulation is not performed. To consider the b-tagging effects, we track all decayed products of b-hadrons after the hadronization. If constituents of a jet inlcude these products, we say that this jet is a true b-jet. Same procedures are applied to label c-jet. Fig. 5 shows the number of true b-jets and c-jets. Obviously, a b-jet and a c-jet are found in the $t\bar{c}(\bar{t}c)$ signal. For backgrounds with two b quarks ($t\bar{t}$ and $b\bar{b}$), two b-jets can be found in most events. For the $c\bar{c}$ backgrounds, most events include two c-jets. ZZ, W^+W^- or $W^{\pm}jj$ can decay to b or c quark, so we also observe some b- or c-jets are found in these events. Most of the $q\bar{q}$ events have not both b- and c-jet, but a small fraction includes b- or c-jet. In the parton shower, quark has probability to radiate a gluon, and this gluon may split to $b\bar{b}(c\bar{c})$. Such kind of process is easier to occur at high energy muon collider, which may increase the mistagging rate of light quarks. With this true flavour information, we can implement a b-tagging cut. In our analysis, the b-tagging rate is $\epsilon_b = 0.7$, while the mistagging rate is $\epsilon_c = 0.1$ and $\epsilon_q = 0.01$ for c-jets and light jets, respectively.

Now we can introduce some cuts to reduce backgrounds:

- Cut1: $N_{jet} = 2$, $N_{lepton} = 0$,
- Cut2: $M_{jj} > 8$ TeV,
- Cut3: 150 GeV$< M(HJ) <$ 200 GeV,

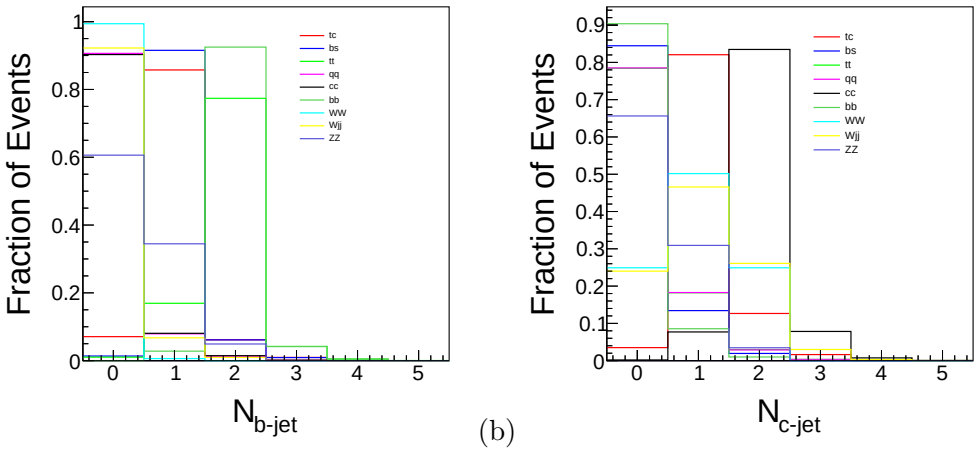

(a) (b)

Figure 5. The number of (a) true b-jet and (b) true c-jet in signal and backgrounds are displayed.

	No Cuts	Cut1	Cut2	Cut3	Cut4	Cut5	S/B	$S/\sqrt{S+B}$
$\mu^+\mu^- \to tc$	2541	1222	1168	740	497	304		
$\mu^+\mu^- \to t\bar{t}$	2.15×10^4	1.03×10^4	9970	7602	269	106		
$\mu^+\mu^- \to q\bar{q}$	1.07×10^5	4.95×10^4	4.93×10^4	5084	3498	224		
$\mu^+\mu^- \to c\bar{c}$	5.19×10^4	2.40×10^4	2.30×10^4	2365	1677	210	0.38	9.12
$\mu^+\mu^- \to b\bar{b}$	2.74×10^4	1.29×10^4	1.12×10^4	1158	829	159		
$\mu^+\mu^- \to W^+W^-$	7.56×10^5	7.18×10^5	7.18×10^5	3555	560	0		
$\mu^+\mu^- \to Wjj$	1.07×10^6	3.49×10^4	3.32×10^4	2929	1811	107		
$\mu^+\mu^- \to ZZ$	4.55×10^4	4.54×10^4	4.49×10^4	0	0	0		

Table 2. The number of events before and after cut are listed. We assume the luminosity is 30 ab^{-1} at 10 TeV muon collider. The details of cuts are described in the text.

- Cut4: $M(LJ) < 75$ GeV,
- Cut5: the heavy jet is b-tagged and the light jet is not tagged.

The cut flows are listed in Table. 2. As we can see, the cuts for jet invariant mass are efficient to reduce backgrounds with heavy particles. The b-tagging cut is efficient to reduce backgrounds with W boson. After these cuts, the huge backgrounds are reduced significantly, and the signal can be observed.

As a reference, we analyze the $\mu^+\mu^- \to b\bar{s}(\bar{b}s)$ with similar method. The cuts we introduce are

- Cut1: $N_{jet} = 2$, $N_{lepton} = 0$,
- Cut2: $M_{jj} > 8$ TeV,
- Cut3: $M(HJ) < 75$ GeV,

	No Cuts	Cut1	Cut2	Cut3	Cut4	S/B	$S/\sqrt{S+B}$
$\mu^+\mu^- \to bs$	4599	2201	2080	927	642		
$\mu^+\mu^- \to t\bar{t}$	2.15×10^4	1.03×10^4	9970	2	2		
$\mu^+\mu^- \to q\bar{q}$	1.07×10^5	4.95×10^4	4.93×10^4	2.14×10^4	1066		
$\mu^+\mu^- \to c\bar{c}$	5.19×10^4	2.40×10^4	2.30×10^4	1.01×10^4	2207	0.08	6.91
$\mu^+\mu^- \to b\bar{b}$	2.74×10^4	1.29×10^4	1.12×10^4	4987	2019		
$\mu^+\mu^- \to W^+W^-$	7.56×10^5	7.18×10^5	7.18×10^5	1.25×10^5	1392		
$\mu^+\mu^- \to Wjj$	1.07×10^6	3.49×10^4	3.32×10^4	1.19×10^4	1118		
$\mu^+\mu^- \to ZZ$	4.55×10^4	4.54×10^4	4.49×10^4	447	188		

Table 3. The number of events before and after cut are listed. We assume the luminosity is 30 ab^{-1} at 10 TeV muon collider. The details of cuts are described in the text.

- Cut4: One jet is b-tagged.

The cut flows are listed in Table. 3. As we dicuss above, heavy jets should be normal at a high energy muon collider. The invariant mass cut is necessary to reject backgrounds like $t\bar{t}$ and ZZ. The remained backgrounds with W boson can be further reduced by b-tagging cut.

5 Summary and Discussion

For the signal processes $\mu^+\mu^- \to bs$ [34], it has been revealed that b tagging is crucial to reject background events from jj final states. The dominant background events are jj. In order to extract the information on the Wilson coefficients C_9 and C_{10}, it is found that the polarized muon beams and the measurement of forward-backward asymmetry of final state is crucial.

In this work, instead of assuming polarized muon beams and charge tagging of final state, we propose to measure the signal processes $\mu^+\mu^- \to tc$. Then it is found that the major task is to reject $t\bar{t}$ and WW events, which might be even easier to pick out signal events. It is also found that the weak radiation jjW is large and might be relevant background.

It is also found that in order to resolve the signal events, detectors with high granuality are needed, since top quarks and W bosons in the hadronic final states are around 5 TeV and are highly boosted objects. In order to capture the substructure of these massive jets, the cone parameter should be set as around $0.09 - 0.1$ when the collision energy is assumed to be $\sqrt{s} = 10$ TeV, which is much smaller compared with the cone parameter adopted as $R = 0.4$ or 0.5 at the LHC. To extract signal events from large background events, refined analysis of jet substructure at TeV region should be applied in order to achieve a much better performance.

To distinguish new physics models, it is found that the measurement of $\mu^+\mu^- \to tc$ can pinpoint the Model I and Model II. Model III can be discovered due to the near resonance near a few TeV region. Model IV could be favored if there is no signal of the process $\mu^+\mu^- \to tc$ can be measured.

Acknowledgments

Z.J. Zhao has been partially supported by a Nikolai Uraltsev Fellowship of the Center for Particle Physics, University of Siegen, and partially supported by the Natural Science Foundation of China under the grant No. 11875260. S.C. Sun is supported by the MOST of Taiwan under grant number of 105-2811-M-002-130 and the CRF Grants of the Government of the Hong Kong SAR under HUKST4/CRF/13G. Q.S. Yan is supported by the Natural Science Foundation of China under the grant No. 11475180 and No. 11875260. X.R. Zhao has received funding from the European Union's Horizon 2020 research and innovation programme as part of the Marie Skłodowska-Curie Innovative Training Network MCnetITN3 (grant agreement no. 722104). We would like to acknowledge the Mainz Institute for Theoretical Physics(MITP) for enabling us to complete this work.

A SMEFT Renormalization Group Equation

The RGE of SMEFT Wilson coefficients can be written as

$$\frac{dC_i}{d\ln\mu} = \frac{1}{16\pi^2}\beta_i. \tag{A.1}$$

All 1-loop β functions of operators in Warsaw basis have been derived in Ref. [55].

The β functions of operators 2.12∼2.14 are

$$\begin{aligned}
\left[\beta_{lq}^{(1)}\right]_{prst} &= \frac{2}{3}g'^2\left([C_{lq}^{(1)}]_{wwst} + [C_{qe}]_{stww}\right)\delta_{pr} - g'^2[C_{lq}^{(1)}]_{prst} \\
&\quad +9g^2[C_{lq}^{(3)}]_{prst} + \frac{1}{2}[\Gamma_u^\dagger\Gamma_u]_{vt}[C_{lq}^{(1)}]_{prsv}, &\text{(A.2)}\\
\left[\beta_{lq}^{(3)}\right]_{prst} &= \frac{2}{3}g^2[C_{lq}^{(3)}]_{wwst}\delta_{pr} + 3g^2[C_{lq}^{(1)}]_{prst} - (6g^2+g'^2)[C_{lq}^{(3)}]_{prst} \\
&\quad +\frac{1}{2}[\Gamma_u^\dagger\Gamma_u]_{vt}[C_{lq}^{(3)}]_{prsv}, &\text{(A.3)}\\
[\beta_{qe}]_{prst} &= \frac{4}{3}g'^2\left([C_{lq}^{(1)}]_{wwpr} + [C_{qe}]_{prww}\right)\delta_{st} + 2g'^2[C_{qe}]_{prst} \\
&\quad +\frac{1}{2}[\Gamma_u^\dagger\Gamma_u]_{vr}[C_{lq}^{(1)}]_{pvst}, &\text{(A.4)}
\end{aligned}$$

where g and g' are the gauge coupling of $SU(2)$ and $U(1)$, respectively. Γ_u is the 3×3 Yukawa mass matrix of u-type quarks. For simplicity, we only consider top quark is massive, and only the element $\Gamma_u(3,3)=1$ is non-zero. Note the Eq. A.2∼A.4 only contain the most important contributions and mixing of the corresponding operators. The mixing of the full set of operators is beyond the scope of this work.

The 1-loop RGE running of SM parameters are given by these β functions:

$$\begin{aligned}
\beta_g &= -\frac{19}{6}g^3, &\text{(A.5)}\\
\beta_{g'} &= \frac{41}{6}g'^3, &\text{(A.6)}\\
\beta_{g_s} &= -7g_s^2, &\text{(A.7)}\\
[\beta_{\Gamma_u}]_{33} &= \frac{9}{4}g^2\Gamma_u(3,3) - \frac{17}{12}g'^2\Gamma_u(3,3) - 8g_s^2\Gamma_u(3,3) + \frac{9}{2}\Gamma_u^3(3,3). &\text{(A.8)}
\end{aligned}$$

Our simplified RGE running has been compared with two tools: DSixTools [55, 56] and Wilson [57]. The differences between our results and these tools are below 1%.

B LEFT Renormalization Group Equation

The definition of RGE of LEFT is the same as Eq. A.1, but C_i are replaced by L_i. The β functions of operator 2.5 and 2.6 are

$$\left[\beta_{ed}^{V,LL}\right]_{prst} = \frac{4}{3}e^2 q_e q_d \delta_{pr}\left([L_{ed}^{V,LL}]_{wwst} + [L_{ed}^{V,LL}]_{stww}\right) + 12e^2 q_e q_d [L_{ed}^{V,LL}]_{prst}, \quad \text{(B.1)}$$

$$\left[\beta_{de}^{V,LR}\right]_{prst} = \frac{4}{3}e^2 q_e^2 \delta_{st}\left([L_{ed}^{V,LL}]_{wwpr} + [L_{de}^{V,LR}]_{prww}\right) - 12e^2 q_e q_d [L_{de}^{V,LR}]_{prst}, \quad \text{(B.2)}$$

where e is the coupling constant of QED. $q_e = -1$ and $q_d = -1/3$ are the charges of lepton and d-type quark, respectively.

At the low energy scale, the 1-loop running of QCD and QED coupling are given by following β functions:

$$\beta_{g_s} = -\frac{23}{3}g_s^3, \quad \text{(B.3)}$$

$$\beta_e = \frac{80}{9}e^3, \quad \text{(B.4)}$$

References

[1] LHCb collaboration, *Measurement of the $B_s^0 \to \mu^+\mu^-$ decay properties and search for the $B^0 \to \mu^+\mu^-$ and $B_s^0 \to \mu^+\mu^-\gamma$ decays*, *Phys. Rev. D* **105** (2022) 012010 [2108.09283].

[2] LHCb collaboration, *Analysis of Neutral B-Meson Decays into Two Muons*, *Phys. Rev. Lett.* **128** (2022) 041801 [2108.09284].

[3] LHCb collaboration, *Measurement of the $B_s^0 \to \mu^+\mu^-$ branching fraction and effective lifetime and search for $B^0 \to \mu^+\mu^-$ decays*, *Phys. Rev. Lett.* **118** (2017) 191801 [1703.05747].

[4] ATLAS collaboration, *Study of the rare decays of B_s^0 and B^0 mesons into muon pairs using data collected during 2015 and 2016 with the ATLAS detector*, *JHEP* **04** (2019) 098 [1812.03017].

[5] CMS collaboration, *Measurement of properties of $B_s^0 \to \mu^+\mu^-$ decays and search for $B^0 \to \mu^+\mu^-$ with the CMS experiment*, *JHEP* **04** (2020) 188 [1910.12127].

[6] LHCb collaboration, *Test of lepton universality in beauty-quark decays*, *Nature Phys.* **18** (2022) 277 [2103.11769].

[7] LHCb collaboration, *Search for lepton-universality violation in $B^+ \to K^+\ell^+\ell^-$ decays*, *Phys. Rev. Lett.* **122** (2019) 191801 [1903.09252].

[8] LHCb collaboration, *Test of lepton universality with $B^0 \to K^{*0}\ell^+\ell^-$ decays*, *JHEP* **08** (2017) 055 [1705.05802].

[9] LHCb collaboration, *Angular analysis of the $B^0 \to K^{*0}\mu^+\mu^-$ decay using 3 fb^{-1} of integrated luminosity*, *JHEP* **02** (2016) 104 [1512.04442].

[10] LHCb collaboration, *Measurement of CP-Averaged Observables in the $B^0 \to K^{*0}\mu^+\mu^-$ Decay*, *Phys. Rev. Lett.* **125** (2020) 011802 [2003.04831].

[11] LHCb collaboration, *Angular Analysis of the $B^+ \to K^{*+}\mu^+\mu^-$ Decay*, *Phys. Rev. Lett.* **126** (2021) 161802 [2012.13241].

[12] G. Hiller and M. Schmaltz, *Diagnosing lepton-nonuniversality in $b \to s\ell\ell$*, *JHEP* **02** (2015) 055 [1411.4773].

[13] W. Altmannshofer, C. Niehoff, P. Stangl and D. M. Straub, *Status of the $B \to K^*\mu^+\mu^-$ anomaly after Moriond 2017*, *Eur. Phys. J. C* **77** (2017) 377 [1703.09189].

[14] W. Altmannshofer and D. M. Straub, *New physics in $b \to s$ transitions after LHC run 1*, *Eur. Phys. J. C* **75** (2015) 382 [1411.3161].

[15] L.-S. Geng, B. Grinstein, S. Jäger, J. Martin Camalich, X.-L. Ren and R.-X. Shi, *Towards the discovery of new physics with lepton-universality ratios of $b \to s\ell\ell$ decays*, *Phys. Rev. D* **96** (2017) 093006 [1704.05446].

[16] M. Ciuchini, A. M. Coutinho, M. Fedele, E. Franco, A. Paul, L. Silvestrini et al., *New Physics in $b \to s\ell^+\ell^-$ confronts new data on Lepton Universality*, *Eur. Phys. J. C* **79** (2019) 719 [1903.09632].

[17] A. Datta, J. Kumar and D. London, *The B anomalies and new physics in $b \to se^+e^-$*, *Phys. Lett. B* **797** (2019) 134858 [1903.10086].

[18] J. Aebischer, W. Altmannshofer, D. Guadagnoli, M. Reboud, P. Stangl and D. M. Straub, *B-decay discrepancies after Moriond 2019*, *Eur. Phys. J. C* **80** (2020) 252 [1903.10434].

[19] M. Ciuchini, M. Fedele, E. Franco, A. Paul, L. Silvestrini and M. Valli, *Lessons from the $B^{0,+} \to K^{*0,+}\mu^+\mu^-$ angular analyses*, *Phys. Rev. D* **103** (2021) 015030 [2011.01212].

[20] S. Jäger, M. Kirk, A. Lenz and K. Leslie, *Charming new physics in rare B-decays and mixing?*, *Phys. Rev. D* **97** (2018) 015021 [1701.09183].

[21] V. Shiltsev and F. Zimmermann, *Modern and Future Colliders*, *Rev. Mod. Phys.* **93** (2021) 015006 [2003.09084].

[22] C. Aime et al., *Muon Collider Physics Summary*, 2203.07256.

[23] Muon Collider collaboration, *The physics case of a 3 TeV muon collider stage*, 2203.07261.

[24] J. P. Delahaye, M. Diemoz, K. Long, B. Mansoulié, N. Pastrone, L. Rivkin et al., *Muon Colliders*, 1901.06150.

[25] T. Han, Z. Liu, L.-T. Wang and X. Wang, *WIMPs at High Energy Muon Colliders*, *Phys. Rev. D* **103** (2021) 075004 [2009.11287].

[26] S. Bottaro, D. Buttazzo, M. Costa, R. Franceschini, P. Panci, D. Redigolo et al., *Closing the window on WIMP Dark Matter*, *Eur. Phys. J. C* **82** (2022) 31 [2107.09688].

[27] D. Buttazzo, R. Franceschini and A. Wulzer, *Two Paths Towards Precision at a Very High Energy Lepton Collider*, *JHEP* **05** (2021) 219 [2012.11555].

[28] A. Costantini, F. De Lillo, F. Maltoni, L. Mantani, O. Mattelaer, R. Ruiz et al., *Vector boson fusion at multi-TeV muon colliders*, *JHEP* **09** (2020) 080 [2005.10289].

[29] M. Chiesa, F. Maltoni, L. Mantani, B. Mele, F. Piccinini and X. Zhao, *Measuring the quartic Higgs self-coupling at a multi-TeV muon collider*, *JHEP* **09** (2020) 098 [2003.13628].

[30] D. Buttazzo and P. Paradisi, *Probing the muon $g-2$ anomaly with the Higgs boson at a muon collider*, *Phys. Rev. D* **104** (2021) 075021 [2012.02769].

[31] R. Capdevilla, D. Curtin, Y. Kahn and G. Krnjaic, *Discovering the physics of $(g-2)_\mu$ at future muon colliders*, *Phys. Rev. D* **103** (2021) 075028 [2006.16277].

[32] R. Capdevilla, D. Curtin, Y. Kahn and G. Krnjaic, *No-lose theorem for discovering the new physics of (g-2)μ at muon colliders*, *Phys. Rev. D* **105** (2022) 015028 [2101.10334].

[33] R. Capdevilla, D. Curtin, Y. Kahn and G. Krnjaic, *Systematically testing singlet models for $(g-2)_\mu$*, *JHEP* **04** (2022) 129 [2112.08377].

[34] W. Altmannshofer, S. A. Gadam and S. Profumo, *Snowmass White Paper: Probing New Physics with $\mu^+\mu^- \to bs$ at a Muon Collider*, in *2022 Snowmass Summer Study*, 3, 2022, 2203.07495.

[35] G.-y. Huang, F. S. Queiroz and W. Rodejohann, *Gauged $L_\mu - L_\tau$ at a muon collider*, *Phys. Rev. D* **103** (2021) 095005 [2101.04956].

[36] I. Doršner, S. Fajfer, A. Greljo, J. F. Kamenik and N. Košnik, *Physics of leptoquarks in precision experiments and at particle colliders*, *Phys. Rept.* **641** (2016) 1 [1603.04993].

[37] E. E. Jenkins, A. V. Manohar and P. Stoffer, *Low-Energy Effective Field Theory below the Electroweak Scale: Operators and Matching*, *JHEP* **03** (2018) 016 [1709.04486].

[38] W. Altmannshofer and P. Stangl, *New physics in rare B decays after Moriond 2021*, *Eur. Phys. J. C* **81** (2021) 952 [2103.13370].

[39] B. Grzadkowski, M. Iskrzynski, M. Misiak and J. Rosiek, *Dimension-Six Terms in the Standard Model Lagrangian*, *JHEP* **10** (2010) 085 [1008.4884].

[40] S. Baek, N. G. Deshpande, X. G. He and P. Ko, *Muon anomalous g-2 and gauged L(muon) - L(tau) models*, *Phys. Rev. D* **64** (2001) 055006 [hep-ph/0104141].

[41] E. Ma, D. P. Roy and S. Roy, *Gauged L(mu) - L(tau) with large muon anomalous magnetic moment and the bimaximal mixing of neutrinos*, *Phys. Lett. B* **525** (2002) 101 [hep-ph/0110146].

[42] P. J. Fox, J. Liu, D. Tucker-Smith and N. Weiner, *An Effective Z'*, *Phys. Rev. D* **84** (2011) 115006 [1104.4127].

[43] W. Altmannshofer, S. Gori, M. Pospelov and I. Yavin, *Quark flavor transitions in $L_\mu - L_\tau$ models*, *Phys. Rev. D* **89** (2014) 095033 [1403.1269].

[44] V. Gherardi, D. Marzocca and E. Venturini, *Matching scalar leptoquarks to the SMEFT at one loop*, *JHEP* **07** (2020) 225 [2003.12525].

[45] M. Bauer and M. Neubert, *Minimal Leptoquark Explanation for the $R_{D^{(*)}}$, R_K , and $(g-2)_\mu$ Anomalies*, *Phys. Rev. Lett.* **116** (2016) 141802 [1511.01900].

[46] R. Barbieri, G. Isidori, A. Pattori and F. Senia, *Anomalies in B-decays and U(2) flavour symmetry*, *Eur. Phys. J. C* **76** (2016) 67 [1512.01560].

[47] D. Buttazzo, A. Greljo, G. Isidori and D. Marzocca, *B-physics anomalies: a guide to combined explanations*, *JHEP* **11** (2017) 044 [1706.07808].

[48] A. Alloul, N. D. Christensen, C. Degrande, C. Duhr and B. Fuks, *FeynRules 2.0 - A complete toolbox for tree-level phenomenology*, *Comput. Phys. Commun.* **185** (2014) 2250 [1310.1921].

[49] J. Alwall, R. Frederix, S. Frixione, V. Hirschi, F. Maltoni, O. Mattelaer et al., *The automated computation of tree-level and next-to-leading order differential cross sections, and their matching to parton shower simulations*, *JHEP* **07** (2014) 079 [1405.0301].

[50] C. Bierlich et al., *A comprehensive guide to the physics and usage of PYTHIA 8.3*, 2203.11601.

[51] M. Cacciari, G. P. Salam and G. Soyez, *FastJet User Manual*, *Eur. Phys. J. C* **72** (2012) 1896 [1111.6097].

[52] S. Catani, Y. L. Dokshitzer, M. Olsson, G. Turnock and B. R. Webber, *New clustering algorithm for multi - jet cross-sections in e+ e- annihilation*, *Phys. Lett. B* **269** (1991) 432.

[53] S. Catani, Y. L. Dokshitzer, M. H. Seymour and B. R. Webber, *Longitudinally invariant K_t clustering algorithms for hadron hadron collisions*, *Nucl. Phys. B* **406** (1993) 187.

[54] S. D. Ellis and D. E. Soper, *Successive combination jet algorithm for hadron collisions*, *Phys. Rev. D* **48** (1993) 3160 [hep-ph/9305266].

[55] A. Celis, J. Fuentes-Martin, A. Vicente and J. Virto, *DsixTools: The Standard Model Effective Field Theory Toolkit*, *Eur. Phys. J. C* **77** (2017) 405 [1704.04504].

[56] J. Fuentes-Martin, P. Ruiz-Femenia, A. Vicente and J. Virto, *DsixTools 2.0: The Effective Field Theory Toolkit*, *Eur. Phys. J. C* **81** (2021) 167 [2010.16341].

[57] J. Aebischer, J. Kumar and D. M. Straub, *Wilson: a Python package for the running and matching of Wilson coefficients above and below the electroweak scale*, *Eur. Phys. J. C* **78** (2018) 1026 [1804.05033].